

RFX1-mediated CCN3 induction that may support chondrocyte survival under starved conditions

Tomomi Mizukawa^{1,2} | Takashi Nishida^{1,3} | Sho Akashi^{1,4} | Kazumi Kawata¹ | Sumire Kikuchi¹ | Harumi Kawaki^{1,5} | Masaharu Takigawa³ | Hiroshi Kamioka² | Satoshi Kubota¹

¹*Department of Biochemistry and Molecular Dentistry, Okayama University Graduate School of Medicine, Dentistry and Pharmaceutical Sciences, Okayama, Japan*

²*Department of Orthodontics, Okayama University Graduate School of Medicine, Dentistry and Pharmaceutical Sciences, Okayama, Japan*

³*Advanced Research Center for Oral and Craniofacial Sciences, Okayama University Dental School, Okayama, Japan*

⁴*Department of Oral and Maxillofacial Reconstructive Surgery, Okayama University Graduate School of Medicine, Dentistry and Pharmaceutical Sciences, Okayama, Japan*

⁵*Department of Oral Biochemistry, Asahi University School of Dentistry, Mizuho, Japan*

Number of figures: 8; one color figure is provided.

Running title: CCN3 induction via RFX-1 by starvation

Corresponding author:

Satoshi Kubota

Department of Biochemistry and Molecular Dentistry, Okayama University Graduate School of Medicine, Dentistry and Pharmaceutical Sciences

2-5-1 Shikata-cho, Kita-ku, Okayama 700-8525, Japan

E-mail: kubota1@md.okayama-u.ac.jp

Abstract

Cellular communication network factor (CCN) family members are multifunctional matricellular proteins that manipulate and integrate extracellular signals. In our previous studies investigating the role of CCN family members in cellular metabolism, we found three members that might be under the regulation of energy metabolism. In this study, we confirmed that CCN2 and CCN3 are the only members that are tightly regulated by glycolysis in human chondrocytic cells. Interestingly, CCN3 was induced under a variety of impaired glycolytic conditions. This CCN3 induction was also observed in two breast cancer cell lines with a distinct phenotype, suggesting a basic role of CCN3 in cellular metabolism. Reporter gene assays indicated a transcriptional regulation mediated by an enhancer in the proximal promoter region. As a result of analyses *in silico*, we specified regulatory factor binding to the X-box (RFX) 1 as a candidate that mediated the transcriptional activation by impaired glycolysis. Indeed, the inhibition of glycolysis induced the expression of *RFX1*, and *RFX1* silencing nullified the CCN3 induction by impaired glycolysis. Subsequent experiments with an anti-CCN3 antibody indicated that CCN3 supported the survival of chondrocytes under impaired glycolysis. Consistent with these findings *in vitro*, abundant CCN3 production by chondrocytes in the deep zones of developing epiphyseal cartilage, which are located far away from the synovial fluid, was confirmed *in vivo*. Our present study uncovered that RFX1 is the mediator that enables CCN3 induction upon cellular starvation, which may eventually assist chondrocytes in retaining their viability, even when there is an energy supply shortage.

KEYWORDS: CCN2, CCN3, glycolysis, metabolism, cartilage

1 | INTRODUCTION

Chondrocytes are key players in the skeletal development of vertebrates, as well as housekeepers of permanent cartilage, such as articular and auricular cartilage. These highly specialized cells are embedded in cartilage, which is an avascular connective tissue with a limited oxygen and nutrient supply. Indeed, the survival strategy under these tough conditions is a critical issue for chondrocytes (Hollander and Zeng, 2019).

In order to survive, chondrocytes need to generate energy. However, due to the limited oxygen in cartilage, ATP production by oxidative phosphorylation in mitochondria is ineffective. Therefore, chondrocytes are forced to depend on glycolysis that can acquire ATP even under anaerobic conditions (Hollander and Zeng, 2019). In comparison with oxidative phosphorylation by mitochondria, direct ATP production by glycolysis is fast, but its production efficiency is poor. As a consequence, a large amount of glucose is required for chondrocytes to obtain a sufficient amount of ATP. However, since cartilage is an avascular connective tissue, no glucose can be supplied to chondrocytes directly from blood. As such, chondrocytes are always under starved conditions.

In this way, a particular system, with which chondrocytes can endure a glucose shortage, should be furnished in these cells in cartilage. Such a system may also be desired for cancer cells. Because of their aggressive cellular activities and dependence on glycolysis, which is entitled the Warburg effect (Liberti & Locasale, 2016), these malignant cells are usually short of glucose, unless they can induce neovascularization.

The cellular communication network factor (CCN) family consists of multifunctional proteins that manipulate extracellular molecular networks (Takigawa, 2017; Perbal, 2018; Perbal et al., 2018). In mammals, it is composed of six members—CCN1 to CCN6—

which have similar structures. CCN family proteins are basically made up of four characteristic modules, which are the insulin-like growth factor binding protein-like (IGFBP) module, von Willebrand factor type C repeat (VWC) module, thrombospondin type 1 repeat (TSP1) module, and C-terminal cystine knot (CT) module (Kubota & Takigawa, 2013). These modules interact with various extracellular molecules, such as growth factors, cell surface receptors, and extracellular matrix (ECM) components (Rachfal & Brigstock 2005). As a result, these proteins manipulate extracellular signal transduction networks to exert various physiological and pathological functions (Kubota & Takigawa 2013). Recent studies have revealed that the CCN family is deeply involved in the development of the skeletal system, circulatory system, hematopoietic system, nervous system, eye, and pancreas. Along with this, it has been revealed that the CCN family is associated with fibrotic diseases, inflammation, malignant tumors, and eye diseases (Leask, 2020). In particular, these family members are believed to play proper roles in endochondral ossification and articular cartilage development, since all of them are differentially expressed in developing cartilage anlage of long bones in mice (Kawaki et al., 2008). Especially, CCN2 plays an important role during endochondral ossification (Takigawa, 2013). In fact, *Ccn2*-null mice were found to exhibit a severe skeletal deformity caused by impaired endochondral ossification (Ivkovic et al., 2003; Kawaki et al., 2008). It has also been shown that CCN2 and its derivative promote the regeneration of damaged articular cartilage (Nishida et al. 2004; Abd El Kader et al. 2014). Interestingly, *Ccn2* deficiency in chondrocytes strongly induces *Ccn3*, which interacts with bone morphogenetic protein 2 and negatively regulates bone formation (Minamizato et al., 2007; Kawaki et al., 2008).

In our previous study, we evaluated the effect of glycolysis inhibition on the gene

expression of all of the family members in human chondrocytic cells, considering the unique avascular microenvironment of cartilage. As a result, we found that the expression of *CCN2* was significantly reduced by a glycolysis inhibitor, while the expression of *CCN3* and *CCN5* was increased. No significant difference was observed in the gene expression levels of other CCN family members (Akashi et al., 2018). Moreover, *CCN3* expression was also induced by glucose starvation, and it was revealed that *CCN3* is under the control of glycolysis activity. Subsequent reporter gene analysis confirmed that the transcriptional activity of a *CCN3* promoter was increased by the glycolysis inhibitor in a dose-dependent manner. Therefore, it was suggested that the induction of *CCN3* expression by glycolysis inhibition is regulated at a transcriptional level via the proximal promoter (Akashi et al., 2018).

In the present study, we first verified the findings above with another glycolytic inhibitor. Thereafter, the enhancer that mediates *CCN3* induction under an impaired glycolytic condition was specified. Furthermore, we identified regulatory factor binding to the X-box (RFX) 1 as the transcription factor involved in this *CCN3* regulation. Cell biological analysis in vitro and the distribution of *CCN3* in mouse cartilage in vivo suggested the physiological significance of this *CCN3* regulatory system during cartilage development.

2 | MATERIALS AND METHODS

2.1 | *Cell culture*

The human chondrocytic cell line HCS-2/8, which was established from a human chondrosarcoma and was known to retain chondrocytic properties (Takigawa et al., 1989),

and two human breast cancer cell lines with a distinct phenotype, consisting of highly invasive MDA-MB-231 and non-invasive MCF7, were employed (Akashi et al., 2020). These cells were maintained at 37 °C in Dulbecco's modified Eagle's medium (D-MEM) supplemented with 10% fetal bovine serum (FBS) in a humidified atmosphere with 5% CO₂.

2.2 | *Inhibition of glycolysis*

Glycolysis was inhibited by three different strategies. Primarily, we utilized sodium fluoride (NaF), which blocks glycolysis by inhibiting a glycolytic enzyme—enolase. The cells were seeded into 6-well plates and allowed to reach confluence. Thereafter, NaF dissolved in phosphate-buffered saline (PBS) was added at a final concentration of 1 or 5 mM, and the cells were then incubated for 12 h. Finally, total RNAs or proteins were extracted and purified from the cells, as described in another subsection.

Glycolysis was pharmacologically inhibited in a distinct step of the series of enzymatic reactions. For this alternative strategy, monoiodoacetic acid (MIA: Sigma-Aldrich, St. Louis, MO, USA), which is known as an inhibitor of glyceraldehyde 3-phosphate dehydrogenase (GAPDH), was used, as previously described (Nishida et al., 2013). The cells were seeded and grown as described above, and MIA in phosphate-buffered saline (PBS) was added at a final concentration of 0, 2, or 4 µg/mL. After the cells were incubated for another 12 h, total RNAs were extracted and purified.

The inhibition of glycolysis by glucose starvation was performed essentially as previously described (Akashi et al., 2018). Briefly, after having been seeded onto 6-well culture plates, HCS-2/8 cells were grown until they reached confluence. After that, the medium was replaced with DMEM with or without D-glucose. Subsequent culture was

continued for 24 or 48 h. Thereafter, RNA extraction from those cells was carried out.

2.3 | *Extraction of RNA and a quantitative real-time reverse transcription polymerase chain reaction (RT-PCR)*

Cellular RNA was extracted and purified from the cells using Isogen (Nippongene, Tokyo, Japan) or RNeasy® Mini Kit (Qiagen, Hilden, Germany), according to the manufacturers' instructions. Then, reverse transcription was performed using the avian myeloblastosis virus reverse transcriptase, with oligo dT as a primer (PrimeScript™ RT reagent Kit, Takara Bio, Shiga, Japan). Quantitative real-time PCR was then performed using the SYBR® Green real-time PCR Master Mix (TOYOBO, Osaka, Japan) and the StepOnePlus™ real-time PCR system (Applied Biosystems, Basel, Switzerland).

The nucleotide sequences of the primers used in this study are as follows: 5'- GCC AAT GAA GCA GCG TTT CCC- 3' (sense) with 5'- CAA TGA GTC CCA TCA CCC ACA CC -3' (antisense) for *CCN1*; 5'- GCA GGC TAG AGA AGC AGA GC -3' (sense) with 5'- ATG TCT TCA TGC TGG TGC AG -3' (antisense) for *CCN2*; 5'- GGA GCG CGC TAT AAA ACC TG -3' (sense) with 5'- TCC CCT CTC GCT TTT ACC AA -3' (antisense) for *CCN3*; 5'- ACA CTC ATT AAG GCA GGG AAG AAG -3' (sense) with 5'- TCA GGA CAC TGG AAG GAC ACG- 3' (antisense) for *CCN4*; 5'- CCC AGT TTT CTG GCC TTG TC -3' (sense) with 5'- AGA AGC GGT TCT GGT TGG AC -3' (antisense) for *CCN5*; 5'- TTA CAT TCA GCC TTG CGA C -3' (sense) with 5'- CAG CAT CTC TTA TCC AAG CAT -3' (antisense) for *CCN6*; and 5'- GAT CAT TGC TCC TCC TGA GC -3' (sense) with 5'- ACT CCT GCT TGC TGA TCC AC -3' (antisense) for *ACTB* (β -actin).

2.4 | Construction of reporter plasmids

The original reporter gene construct employed to evaluate the promoter activity of human *CCN3* (from -1403 to -45, counted from the translation initiation site) was constructed for our previous work, using pGL3-control (Promega, Madison, WI, USA) as a backbone (Akashi et al., 2018). To make a deletion mutant of the human *CCN3* promoter, this reporter construct was used as a template, and three deletion mutants of the human *CCN3* proximal promoter were prepared by PCR using specific primers. The nucleotide sequences of the primers used were as follows: 5'-TGC TGG GGA CAG ATG AGG TA-3' (sense) and 5'- TCT CCT TAG GGC GCG G-3' (antisense) for deletion mutant 1 (from -1403 to -236); 5'-TGT GTG TGT GTG TGT GTT TT-3' (sense) and 5'-TGT AGA TTG GCA CTG CTC GC-3' (antisense) for deletion mutant 2 (from -853 to -45); and 5'- TGT GTG TGT GTG TGT GTT TT-A-3' (sense) and 5'-TCT CCT TAG GGC GCG G-3' (antisense) for deletion mutant 3 (from -853 to -236). The amplified fragment was subcloned into a pGEM-T easy vector (Promega), and digested by both *Kpn* I and *Sac* I. Then, each *Kpn* I-*Sac* I fragment was ligated into the corresponding sites of the pGL3-control lacking the simian virus 40 (SV40) promoter (pGL3 Δ P). The identity of these three human *CCN3* fragments was confirmed by DNA sequencing.

2.5 | Reporter gene assay

HCS-2/8 cells were seeded into 24-well plates and were cultured until 60-70% confluence in DMEM containing 10% FBS. Thereafter, the medium was refreshed immediately before the plasmid DNA transfection. Four firefly luciferase reporter constructs containing the human *CCN3* promoter fragments described in the previous subsection were transfected into the HCS-2/8 cells, together with a herpes simplex virus

TK promoter-driven *Renilla* luciferase construct (pRL-TK), as an internal control. The cells were transfected with each plasmid in the presence of an optimized amount of FuGENE 6 (Roche). Twenty-four hours after DNA transfection, 4 µg/mL of MIA was added, and incubation was continued for 12 h. Thereafter, the cell lysates were harvested in Passive Lysis Buffer (Promega). Firefly and *Renilla* luciferase activities in cell lysates were measured by the Dual Luciferase system (Promega), and computation of the relative ratios was carried out with a luminometer (Fluoroskan Ascent FL, Labsystems, Helsinki, Finland). All transfection experiments were performed in quadruplicate (El-Seoudi et al., 2017).

2.6 | Screening of transcriptional factors in silico

Prediction of the transcription factors that could bind to the enhancer region in the *CCN3* proximal promoter in silico was performed by the TFBIND program online (<http://tfbind.hgc.jp>), based on the algorithm constructed by Tsunoda and Takagi (Tsunoda & Takagi, 1999). Datasets of chromatin immunoprecipitation-sequencing (ChIP-seq) experiments targeting transcription factors, including RFX1 in MCF7 cells (ENCSR788XNX) in the ENCODE portal (<https://www.encodeproject.org/>) (Sloan et al. 2016), were analyzed to select the candidate among those that were predicted. The expression of *CCN3* in human knee joint articular chondrocytes was also confirmed by the analysis of total RNA sequencing datasets therein (ENCSR000CUE). These datasets were analyzed and visualized by the University of California Santa Cruz (UCSC) Genome Browser (<http://genome.ucsc.edu>).

2.7 | Gene silencing

A small interfering RNA (siRNA) cocktail, consisting of a pool of three target-specific siRNAs against human RFX-1 (sc-37741) and a non-targeting control (sc-37007) were obtained from Santa Cruz Biotechnology, Inc. (Santa Cruz, CA, USA), and gene silencing was performed as described previously (Nishida et al., 2017). Briefly, HCS-2/8 cells were collected after they had reached confluence and were re-suspended in Nucleofactor solution (Lonza Cologne GmbH, Cologne, Germany) containing 100 pmol siRNA against RFX1 or non-targeting control siRNA. Electroporation was performed using an Amaxa™ Human Chondrocyte Nucleofector™ kit and Amaxa Nucleofector1 II (Lonza Cologne GmbH), according to the manufacturer's instructions.

2.8 | Western blotting

After HCS-2/8 cells had been knocked down by the siRNAs against RFX-1, they were treated with NaF at the concentration of 5 mM for 16 h. Then, cell lysates were collected, and Western blot analysis was performed, as described previously (Sumiyoshi et al., 2013). In brief, after protein concentrations of cell lysates had been determined by the Pierce™ BCA Protein Assay using bovine serum albumin (BSA) standards (Thermo Scientific, Rockford, IL, USA), each cell lysate containing an equal amount of proteins was separated by sodium dodecyl sulfate polyacrylamide gel electrophoresis (SDS-PAGE) and was then transferred to polyvinylidene difluoride (PVDF) membranes (Millipore) by using a semi-dry transfer apparatus (Atto Corp., Tokyo, Japan). The blot was reacted with anti-CCN3 (CST, Beverly, MA, USA; Cat # 8767S) and anti-β-actin (Sigma-Aldrich; Cat# A2228) antibodies overnight at 4 °C. After being washed with Tris-buffered saline (TBS)-Tween 20 (TBST) and TBS buffers, the blots were incubated for 60 min at room temperature in secondary antibodies conjugated with horseradish

peroxidase (HRP). Subsequently, the membranes were washed with TBST and TBS buffers, and the bands were detected with the chemiluminescence substrate by using a LAS-4000 mini image analyzer (Fuji Film, Tokyo, Japan).

2.9 | *Cell viability assay*

To evaluate the cell viability after NaF exposure, we performed a WST-8 assay (Dojindo, Kumamoto, Japan). Briefly, HCS-2/8 cells were inoculated into 96-well multiplates and were cultured until they became sub-confluent. Then, these cells were treated with anti-CCN3 (abcam ab137677) and non-immune IgG at the concentration of 5 µg/mL. After 24 h, HCS-2/8 cells were treated with NaF (5 mM) for 24 h, and WST-8 was added to the cultures. These cells were further cultured for 1.5 h and optical absorbance at a wavelength of 450 nm was measured by a microplate reader (SH-1000, CORONA ELECTRIC; Tokyo, Japan).

2.10 | *Immunohistochemistry*

Immunohistochemical staining was performed following an established protocol (Kawaki et al., 2008) under the approval of The Animal Committee of Okayama University Graduate School of Medicine, Dentistry and Pharmaceutical Sciences. In brief, knee joints obtained from BALB c mice on embryonic day 16 were decalcified and embedded in paraffin. Sagittal sections with a 5 µm thickness were prepared with a microtome. The sections were deparaffinized and immersed in ethanol and methanol. After endogenous peroxidase activity was quenched in 3% H₂O₂/methanol, the samples were rehydrated in a serial ethanol dilution. Antigen retrieval was performed with a microwave oven. Before the antibody reaction, the sections were blocked in Histofine

Blocking Agent (Nichirei Biosciences, Tokyo, Japan). An antibody against CCN3—sc-18678 (Santa Cruz Biotechnology, Santa Cruz, CA, USA)—was used to detect CCN3 at the concentration recommended by the manufacturer. Signals were developed by the Histofine Mouse Stain Kit (Nichirei Biosciences) with 3,3'-deaminobenzidine. Counter staining was performed with methyl green.

2.11 | *Statistical Analysis*

Statistical analyses of two experimental groups were performed by using Student's *t*-test, and multiple comparisons among more than two groups were performed by Tukey's and Williams' multiple comparison tests.

3 | RESULTS

3.1 | *Effects of NaF on the gene expression of all of the CCN family members in human chondrocytic cells*

According to our previous study, *CCN2* expression was repressed, and the expression of *CCN3* and *CCN5* was contrarily induced by MIA, which inhibits GAPDH, in human chondrocytic cells (Akashi et al., 2018). In order to further examine whether the observed regulation of CCNs resulted from a glycolysis blockade, we also conducted experiments with other glycolytic inhibition methods. The first method was the inhibition of enolase, which is another enzyme required for glycolysis, by NaF, and the second method was glucose starvation. We added NaF to sub-confluent HCS-2/8 cells and examined the gene expression levels of CCNs by real-time PCR. As a result, it was confirmed that *CCN2* gene expression was markedly decreased, whereas *CCN3* gene

expression was increased, by NaF treatment. However, the increased expression of CCN5 seen with MIA treatment (Akashi et al., 2018) was not recaptured with NaF (Figure 1).

3.2 | Differential regulation of CCN2 and CCN3 under starved conditions in human chondrocytic cells

The results in Figure 1 suggest the repression of CCN2 and induction of CCN3 produced by the inhibition of glycolysis. Consistent with these findings, we had already confirmed CCN3 induction by glucose starvation in a previous study. Therefore, we also evaluated the effect of glucose starvation on CCN2 expression in HCS-2/8 cells. As expected, we found CCN2 repression under a glucose starved condition (Figure 2a). Next, we repeated the experiments with NaF and confirmed a dose-dependent induction of CCN3 (Figure 2b). Finally, the effect of MIA, which inhibits glycolysis in a manner distinct from that of NaF, on CCN2 and CCN3 expression was reevaluated. As shown in Figure 2c, we could successfully reproduce the CCN2 repression and CCN3 induction in HCS-2/8 cells by MIA treatment. Here, we firmly confirmed CCN2 repression and CCN3 induction under a starved condition in chondrocytic HCS-2/8 cells in three distinct strategies (Figure 2d).

3.3 | Induction of CCN3 by glycolysis inhibition in human breast cancer cells

Concerning the two CCN family members under the regulation of glycolysis, our recent study revealed that the positive regulation of CCN2 by glycolytic activity was observed specifically in chondrocytic cells (Akashi et al., 2020). In contrast, negative CCN3 regulation by glycolytic activity was suggested in another cell line. To further

examine whether this *CCN3* regulation system is commonly active among cells with a distinct background, we evaluated the gene expression level of *CCN3* in the absence or presence of MIA or NaF in two human breast cancer cell lines with a distinct phenotype: MDA-MB-231 and MCF7 (Akashi et al., 2020). As a result, the expression of *CCN3* was promoted by MIA and NaF in both cell lines (Figure 3). These results were indeed comparable to those seen with chondrocytic HCS-2/8 cells (Figure 2b and c). Therefore, this *CCN3* regulation by glycolysis is not chondrocyte-specific, but could be a common regulatory system shared by different types of cells.

3.4 | Functional mapping of the enhancer region that mediates *CCN3* regulation by impaired glycolysis

It is known that *CCN3* induction by glycolysis inhibition is conducted at a transcriptional level via the genetic events around the proximal promoter area (Akashi et al., 2018). As a next step in clarifying the mechanism of *CCN3* regulation, four types of reporter plasmids were prepared. In these molecular constructs, three distinct human *CCN3* gene proximal promoter fragments were inserted upstream of the luciferase gene, in order to estimate the enhancer region that mediates the induction of *CCN3* expression by glycolytic inhibition. Full length (FL) contained the -1403 to -45 bp region, deletion mutant 1 (M1) contained the -1403 to -236 bp region, deletion mutant 2 (M2) contained the -853 to -45 bp region, and deletion mutant 3 (M3) contained the -853 to -236 bp region from the translation initiation site. We transfected HCS-2/8 cells with each reporter plasmid, and then treated the cells with MIA. The result of the reporter gene assay showed that FL and M2 responded to MIA, showing increased luciferase activities with MIA (Figure 4a). These results suggest the involvement of an MIA-responsive enhancer

in the region from -236 to -45 bp in the proximal promoter of *CCN3*.

3.5 | Identification of RFX1 as a transcription factor that binds to the CCN3 enhancer and is induced by glycolysis inhibition

As an initial step in specifying transcription factor candidates, we predicted transcription factors, which may bind to the enhancer region of human *CCN3*, based on the nucleotide sequence, by using TFbind software in silico. The TFbind algorithm picked up a number of possible transcription factors as the candidates, as summarized in Figure 4b. Next, in order to identify a transcription factor that actually binds to the enhancer in *CCN3* among these candidates, a few datasets were downloaded from the ENCODE portal site and were analyzed on the UCSC Genome Browser. In these analyses in silico, the expression of *CCN3* in human articular chondrocytes was confirmed (Figure 5a); however, no transcription factor-ChIP (TF-ChIP) dataset from human normal chondrocytes was available. Instead, we analyzed a TF-ChIP dataset from MCF7 breast cancer cells, in which the same *CCN3* regulation by glycolysis was confirmed (Figure 3). Consequently, regulatory factor X (RFX) 1 was found to bind to the *CCN3* enhancer in MCF7 cells (Figure 5a). Thereafter, we examined the effect of glycolysis inhibition on the expression of this transcription factor gene. Interestingly, *RFX1* expression was strongly induced by either MIA or NaF, in a manner comparable to *CCN3* (Figure 5b). Despite no statistical significance being found, *RFX1* expression also exhibited a tendency to respond to glucose starvation (Figure 5c). These findings collectively suggest RFX1 as a glycolysis-sensitive regulator of *CCN3*.

3.6 | Functional requirement of RFX1 for CCN3 regulation by glycolytic activity

Since experiments in silico strongly indicated that RFX1 could mediate *CCN3* regulation by glycolysis, we subsequently examined the role of RFX1 in this *CCN3* regulation by an RNA silencing strategy. First, we transfected RFX1 siRNA into HCS-2/8 cells by electroporation, added NaF 24 hours later, and extracted RNAs 16 hours later for quantitative RT-PCR analysis (Figure 6a), and then confirmed that the gene expression level of RFX1 was reduced to approximately 1/5. Next, we examined the effect of MIA on *CCN3* expression under this RFX1-silenced condition. As a result of *CCN3* gene silencing by siRFX1, induction of the *CCN3* gene was no longer observed in HCS-2/8 cells (Figure 6b). At the protein level, the addition of NaF to HCS-2/8 cells with a non-targeting control siRNA increased *CCN3* production, whereas the induction of *CCN3* production was not observed after the introduction of siRFX1 (Figure 6c). These results indicate that RFX1 is required for the induction of *CCN3* expression and *CCN3* production upon glycolysis inhibition.

3.7 | Reduction of the viability by an antibody against CCN3 in HCS-2/8 cells under impaired glycolysis

Finally, to estimate the cell biological role of *CCN3* produced upon glycolysis inhibition, the viability of NaF-treated HCS-2/8 cells was monitored, in the presence or absence of an antibody which captures *CCN3*. Even when HCS-2/8 cells were treated with NaF, the viability of these cells was still retained at a certain level. However, the addition of an antibody against *CCN3* strongly attenuated the viability of HCS-2/8 cells in the presence of NaF (Figure 7). As such, it was indicated that *CCN3* plays a significant role in supporting the viability of HCS-2/8 cells under starved conditions.

3.8 | *CCN3* production by developing epiphyseal chondrocytes in vivo

In order to confirm the physiological role of the CCN3 regulated by starvation, CCN3 production in mouse cartilage was investigated by immunohistochemical analysis. On embryonic day 16 before secondary ossification center formation, epiphyseal cartilage in mouse knee joints is entirely composed of cartilaginous tissues, with no blood vessels. Therefore, nutrition is supplied to chondrocytes by the synovial fluid infiltrating from the surface of the condyle. As expected, immunohistochemical staining of CCN3 revealed that chondrocytes at the surface with direct contact with synovial fluid showed no CCN3 signals, whereas those in deeper zones with a lower nutrition supply were found to produce CCN3 (Figure 8a). These findings suggest a physiological role of the *CCN3* regulatory system clarified here in vitro in developing cartilage in vivo.

4 | DISCUSSION

The metabolic regulation of CCN2 and CCN3 in chondrocytes represents the critical roles of these proteins in cartilage biology, since both are differentially produced during endochondral ossification, playing distinct roles therein. Of note, glycolysis is severely impaired in *Ccn2*-null growth plate chondrocytes (Maeda-Uematsu et al., 2014), and a strong induction of *Ccn3* expression is observed in these *Ccn2*-null chondrocytes (Kawaki et al., 2008). Therefore, the CCN3 regulatory system uncovered here in chondrocytic HCS-2/8 cells is also active in growth plate chondrocytes in vivo. In contrast to CCN2, CCN3 is produced by chondrocytes in the deep zone of developing epiphysial cartilage (Figure 8a) and quiescent resting chondrocytes in the growth plate (Kawaki et al., 2008), which are located far from synovial fluid and blood vessels and

have a poor nutrition supply. Importantly, our previous study showed that CCN3 repressed the proliferation of growth plate chondrocytes (Kawaki et al., 2008). Therefore, CCN3 induced by the starved condition in these chondrocytes plays a critical role in maintaining chondrocytes in the resting stage, repressing their proliferation and promoting their survival (Figure 8b).

We further confirmed that the CCN3 induction system is utilized in breast cancer cells. Breast cancer cells are totally different from chondrocytes; however, these cells are supposed to utilize this system for different objectives. Tumor cells consume more energy than normal cells, since they are continuously proliferating and expanding. Moreover, their energy production highly depends on glycolysis, which is a result of the Warburg effect (Liberti & Locasale, 2016). As such, tumor cells always have a glucose supply shortage. In order to overcome this glucose shortage, tumor cells perform angiogenesis in order to secure the nutrition supply route. Therefore, cancer cells secrete a number of angiogenic factors, as represented by the vascular endothelial growth factor, to create new blood vessels by stimulating the proliferation of vascular endothelial cells nearby. At the same time, cancer cells release enzymes, which decompose the surrounding connective tissue to guide the neovasculature toward the cancer tissue. Here, we should note that CCN3 also has an angiogenic function (Lin et al., 2005; Kubota & Takigawa, 2007; Henrot et al., 2020). As stated above, the induction of CCN3 under starvation in chondrocytes is postulated to be a protective response. On the other hand, the purpose of CCN3 induction in breast cancer cells could be aggressive; those cells produce CCN3 to secure a glucose supply channel by its angiogenic action for their expansion.

In this study, for the first time, we identified RFX1 as a transcription factor mediating

CCN3 induction upon starvation. RFX1 is a member of the RFX transcription factor family that is widely conserved among animal species. In fact, *Caenorhabditis elegans* and *Drosophila melanogaster* possess one and two RFX genes in their genome, respectively, whereas mammals, including humans, have eight family members (Sugiaman-Trapman et al., 2018). These genes encode transcription factors with a distinct wing-helix type DNA binding domain. RFX transcription factors are involved in a variety of cellular and developmental processes in humans, particularly in relation to ciliogenesis on the surface of polarized cells (Elkon et al., 2015; Tammimies et al., 2016). Therefore, RFX family members are thought to play critical roles in the development and maintenance of human life. It is also of interest that RFX1 expression was found to be correlated with breast cancer prognosis (Shibata et al., 2017).

As the first member of this family, RFX1 is characterized by the retention of both transcriptional activation and repression domains, which may neutralize each other (Sugiaman-Trapman et al., 2018). Indeed, RFX1 was found to activate hepatitis B virus gene expression, whereas it represses *c-myc*, depending upon the promoter context (Lubelsky & Shaul, 2019). Therefore, it is assumed that RFX1 activates *CCN3* in collaboration with other transcription co-factors recruited therein. Since RFX1 expression itself is activated by glycolysis inhibition, the involvement of an upstream regulator of RFX1 is indicated. However, little is known about the factors that regulate RFX1. Although SP2 and ESR1 were indicated to regulate the RFX family of genes, no significant effect of silencing these genes on RFX1 expression was confirmed (Sugiaman-Trapman et al., 2018). In order to clarify the entire system sensing glycolytic activity for the regulation of *CCN3*, further investigation is required.

For the inhibition of glycolysis, MIA was used in vitro in this study. It should be

noted that this chemical compound is usually used for the creation of osteoarthritic lesions in rat joints (Abd El Kader et al., 2014). Osteoarthritis (OA) is an age-related degenerative joint disease characterized by articular cartilage destruction and synovial inflammation. According to epidemiological studies, OA affects half of the world's population over the age of 65 and is one of the most common causes of pain and disability among the elderly (O'Neill et al., 2018). Moreover, the incidence and prevalence of OA have increased significantly over the last few decades, along with the extension of life expectancy. OA is considered to be a multifactorial disease, in which articular cartilage is degenerated by uncontrolled protein degradation by physical, chemical and biological factors. In relation to this disease, previous studies have reported the possible utility of CCN3 in OA therapeutics (Janune et al., 2011 & 2017; Huang et al., 2019). According to a previous report, CCN3 retained in rat articular cartilage was immediately lost in this MIA-induced rat OA model (Janune et al., 2017). This finding in vivo does not contradict our present result in vitro. Since CCN3 is a matricellular protein, it is stably retained in the cartilaginous extracellular matrix (ECM) under healthy conditions. Therefore, upon the loss of ECM, CCN3 is released away from cartilage. Moreover, it is known that CCN3 is a substrate of several matrix metalloproteases (Butler et al., 2017), a few of which are involved in OA development. Under such conditions in vivo, chondrocytes try to supply CCN3. We observed that clustering chondrocytes formed after MIA application produced CCN3 de novo by immunohistochemical analysis (data not shown).

The fact that CCN3 is induced by impaired glycolysis suggest its specific role in survival under starved conditions. Indeed, the viability of chondrocytic cells with impaired glycolysis was reduced by the addition of an antibody against CCN3. CCN3

is capable of changing the behavior of the cells. Our previous studies indicate that CCN3 represses the proliferation of chondrocytes, but promotes their maturation and senescence (Kawaki et al., 2008; Janune et al., 2011, Kuwahara et al., 2020). Most interestingly, another study clarified that CCN3 rapidly recruits hematopoietic stem cells without cell proliferation or self-renewal (Gupta et al., 2005; Ishihara et al., 2014). Therefore, CCN3 may not only recruit these cells, but also lead them to a quiescent stage, in order to optimize metabolic activities and avoid cell death in the recruited microenvironment, as suggested in chondrocytes (Figure 8b). A subsequent study to further clarify the metabolic function of CCN3 is currently in progress.

ACKNOWLEDGMENTS

The authors gratefully thank Drs. Takako Hattori and Eriko Aoyama for their helpful support in experiments, Drs. Michael Snyder and Thomas Gingeras for depositing their data to the ENCODE database, and Ms. Yoshiko Miyake for her secretarial assistance. This study was supported by JSPS KAKENHI Grant Numbers JP17K19756, JP17K19757, JP19H03817, JP19K22716 and JP20K20611.

CONFLICTS OF INTEREST

The authors have nothing to declare.

DATA AVAILABILITY

The data that support the findings of this study are available from the corresponding

author upon reasonable request. Datasets analyzed in this study (ENCSR788XNX and ENCSR000CUE) are available in the ENCODE portal (<https://www.encodeproject.org/>).

REFERENCES

- Abd El Kader, T., Kubota, S., Nishida, T., Hattori, T., Aoyama, E., Janune, D., Hara, E.S., Ono, M., Tabata, Y., Kuboki, T., & Takigawa, M. (2014). The regenerative effects of CCN2 independent modules on chondrocytes in vitro and osteoarthritis models in vivo. *Bone*, *59*, 180-188.
- Akashi, S., Nishida, T., El-Seoudi, A., Takigawa, M., Iida, S., & Kubota, S. (2018). Metabolic regulation of the CCN family genes by glycolysis in chondrocytes. *Journal of Cell Communication & Signaling*, *12*, 245-252.
- Akashi, S., Nishida, T., Mizukawa, T., Kawata, K., Takigawa, M., Iida, S., & Kubota, S. (2020). Regulation of cellular communication network factor 2 (CCN2) in breast cancer cells via the cell-type dependent interplay between CCN2 and glycolysis. *Journal of Oral Biosciences*, *62*, 280-288.
- Butler, G.S., Connor, A.R., Sounni, N.E., Eckhard, U., Morrison, C.J., Noël, A., & Overall, C.M. (2017). Degradomic and yeast 2-hybrid inactive catalytic domain substrate trapping identifies new membrane-type 1 matrix metalloproteinase (MMP14) substrates: CCN3 (Nov) and CCN5 (WISP2). *Matrix Biology*, *59*, 23-38.
- Elkon, R, Milon, B, Morrison, L, Shah, M, Vijayakumar, S., Racherla, M., Leitch, C.C., Silipino, L., Hadi, S., Weiss-Gayet, M., Barras, E., Schmid, C.D., Ait-Lounis, A., Barnes, A., Song, Y., Eisenman, D.J., Eliyahu, E., Frolenkov, G.I., Strome, S.E., Durand, B., Zaghoul, N.A., Jones, S.M., Reith, W., & Hertzano, R. (2015). RFX transcription factors are essential for hearing in mice. *Nature Communications*, *6*, 8549.
- El-Seoudi A, Abd El Kader T, Nishida T, Eguchi T, Aoyama E, Takigawa M, Kubota S.

- (2017) Catabolic effects of FGF-1 on chondrocytes and its possible role in osteoarthritis. *Journal of Cell Communication & Signaling*, *11*, 256-263.
- Gupta, R., Turati, V., Brian, D., Thrussel, C., Wilbourn, B., May, G., & Enver, T. (2005). Nov/CCN3 Enhances Cord Blood Engraftment by Rapidly Recruiting Latent Human Stem Cell Activity. *Cell Stem Cell*, *26*, 527-541
- Henrot, P., Moisan, F., Laurent, P., Manicki, P., Kaulanjan-Checkmodine, P., Jolivel, V., Rezvani, H.R., Leroy, V., Picard F., Boulon, C., Schaeverbeke, T., Seneschal, J., Lazaro, E., Taïeb, A., Truchetet, M.E., & Cario, M. (2020). Decreased CCN3 in systemic sclerosis endothelial cells contributes to impaired angiogenesis. *Journal of Investigative Dermatology*, *140*, 1427-1434.
- Hollander, J.M., & Zeng, L. (2019). The emerging role of glucose metabolism in cartilage development. *Current Osteoporosis Reports*, *17*, 59-69.
- Huang, X., Ni, B., Mao, Z., Xi, Y., Chu, X., Zhang, R., Ma, X., & You H. (2019). NOV/CCN3 induces cartilage protection by inhibiting PI3K/AKT/mTOR pathway. *Journal of Cellular & Molecular Medicine*, *23*, 7525-7534.
- Ishihara, J., Umemoto, T., Yamato, M., Shiratsuchi, Y., Takaki, S., Petrich, B.G., Nakauchi, H., Eto, K., Kitamura, T., & Okano, T. (2014). Nov/CCN3 regulates long-term repopulating activity of murine hematopoietic stem cells via integrin $\alpha\beta 3$. *International Journal of Hematology*, *99*, 393-406.
- Ivkovic, S., Yoon B.S., Popoff, S.N., Safadi, F.F., Libuda, D.E., Stephenson, R.C., Daluiski, A., & Lyons, K.M. (2003). Connective tissue growth factor coordinates chondrogenesis and angiogenesis during skeletal development. *Development*, *130*, 2779-2791.
- Janune, D., Kubota, S., Lazar, N., Perbal, B., Iida, S., & Takigawa, M. (2011). CCN3-

- mediated promotion of sulfated proteoglycan synthesis in rat chondrocytes from developing joint heads. *Journal of Cell Communication & Signaling*, 5, 167-171.
- Janune, D, Abd El Kader, T., Aoyama E., Nishida, T., Tabata, Y., Kubota, S., & Takigawa, M. (2017). Novel role of CCN3 that maintains the differentiated phenotype of articular cartilage. *Journal of Bone & Mineral Metabolism*, 35, 582-597.
- Kawaki, H., Kubota, S., Suzuki, A., Lazar, N., Yamada, T., Matsumura, T., Ohgawara, T., Maeda, T., Perbal, B., Lyons, K.M., & Takigawa M. (2008). Cooperative regulation of chondrocyte differentiation by CCN2 and CCN3 shown by a comprehensive analysis of the CCN family proteins in cartilage. *Journal of Bone and Mineral Research*, 23, 1751-1764.
- Kubota S, & Takigawa M. (2007). CCN family proteins and angiogenesis: from embryo to adulthood. *Angiogenesis*, 10, 1-11.
- Kubota S, Takigawa M. (2011) The role of CCN2 in cartilage and bone development. *Journal of Cell Communication & Signaling*, 5, 209-217.
- Kubota, S., & Takigawa, M. (2013). The CCN family acting throughout the body: recent research developments. *Biomolecular Concepts*, 4, 477-494.
- Kubota S, Takigawa M. (2015) Cellular and molecular actions of CCN2/CTGF and its role under physiological and pathological conditions. *Clinical Science (London)*, 128:181-196.
- Kuwahara M, Kadoya K, Kondo S, Fu S, Miyake Y, Ogo A, Ono M, Furumatsu T, Nakata E, Sasaki T, Minagi S, Takigawa M, Kubota S, Hattori T. (2020). CCN3 (NOV) drives degradative changes in aging articular cartilage. *International Journal of Molecular Sciences*, 21, 7556.
- Leask, A. (2020). Conjunction junction, what's the function? CCN proteins as targets in

- fibrosis and cancers. *American Journal of Physiology - Cell Physiology*, 318, C1046-C1054.
- Liberti, M.V., & Locasale, J.W. (2016). The Warburg effect: How does it benefit cancer cells? *Trends in Biochemical Sciences*, 41, 211-218.
- Lin, C.G., Chen, C.C., Leu, S.J., Grzeszkiewicz, T.M., & Lau, L.F. (2005). Integrin-dependent functions of the angiogenic inducer NOV (CCN3): implication in wound healing. *Journal of Biological Chemistry*, 280, 8229-37.
- Lubelsky, Y., & Shaul, Y. (2019). Recruitment of the protein phosphatase-1 catalytic subunit to promoters by the dual-function transcription factor RFX1. *Biochemical & Biophysical Research Communications*, 509, 1015-1020.
- Maeda-Uematsu, A., Kubota, S., Kawaki, H., Kawata, K., Miyake, Y., Hattori, T., Nishida, T., Moritani, N., Lyons, K.M., Iida, S., & Takigawa, M. (2014). CCN2 as a novel molecule supporting energy metabolism of chondrocytes. *Journal of Cellular Biochemistry*, 115, 854-865.
- Minamizato, T., Sakamoto, K., Liu, T., Kokubo, H., Katsube, K., Perbal, B., Nakamura, S., & Yamaguchi, A. (2007). CCN3/NOV inhibits BMP-2-induced osteoblast differentiation by interacting with BMP and Notch signaling pathways. *Biochemical & Biophysical Research Communications*, 354, 567-73.
- Nishida, T., Kubota, S., Kojima, S., Kuboki, T., Nakao, K., Kushibiki, T., Tabata, Y., & Takigawa, M. (2004). Regeneration of defects in articular cartilage in rat knee joints by CCN2 (connective tissue growth factor), *Journal of Bone & Mineral Research*, 19, 1308-1319.
- Nishida, T., Kubota, S., Aoyama, E., & Takigawa, M. (2013). Impaired glycolytic metabolism causes chondrocyte hypertrophy-like changes via promotion of phospho-

- Smad1/5/8 translocation into nucleus. *Osteoarthritis and Cartilage*, 21, 700-709.
- Nishida, T., Kubota, S., Aoyama, E., Yamanaka N., Lyons, K.M., & Takigawa, M. (2017). Low-intensity pulsed ultrasound (LIPUS) treatment of cultured chondrocytes stimulates production of CCN family protein 2 (CCN2), a protein involved in the regeneration of articular cartilage: mechanism underlying this stimulation. *Osteoarthritis and Cartilage*, 25, 759-769.
- O'Neill, T.W., McCabe, P.S., & McBeth, J. (2018). Update on the epidemiology, risk factors and disease outcomes of osteoarthritis. *Best Practice & Research Clinical Rheumatology*, 32, 312-326.
- Perbal, B. (2018). The concept of the CCN protein family revisited: a centralized coordination network. *Journal of Cell Communication & Signaling*, 12, 3-12.
- Perbal, B., Tweedie, S., & Bruford, E. (2018) The official unified nomenclature adopted by the HGNC calls for the use of the acronyms, CCN1-6, and discontinuation in the use of CYR61, CTGF, NOV and WISP 1-3 respectively, *Journal of Cell Communication & Signaling*, 12, 625-629.
- Rachfal AW, Brigstock DR. (2005) Structural and functional properties of CCN proteins, *Vitamins & Hormones*, 70:69-103.
- Shibata, M., Kanda, M., Shimizu, D., Tanaka, H., Umeda, S., Hayashi, M., Inaishi, T., Miyajima, N., Adachi, Y., Takano, Y., Nakanishi, K., Takeuchi, D., Noda, S., Kodera, Y., & Kikumori, T. (2017). Expression of regulatory factor X1 can predict the prognosis of breast cancer. *Oncology Letters*, 13, 4334-4340.
- Sloan, C.A., Chan, ET., Davidson, J.M., Malladi, V.S., Strattan, J.S., Hitz, B.C., Gabdank, I., Narayanan, A.K., Ho, M., Lee, B.T., Rowe, L.D., Dreszer, T.R., Roe, G., Podduturi, N.R., Tanaka, F., Hong, E.L., & Cherry, J.M. (2016). ENCODE data at the ENCODE

- portal. *Nucleic Acids Research*, 44, D726-732.
- Sugiaman-Trapman, D., Vitezic, M., Jouhilahti, E.M., Mathelier, A., Lauter, G., Misra, S., Daub, C.O., Kere, J., & Swoboda, P. (2018). Characterization of the human RFX transcription factor family by regulatory and target gene analysis. *BMC Genomics*, 19, 181.
- Sumiyoshi K, Kubota S, Ohgawara T, Kawata K, Abd El Kader T, Nishida T, Ikeda N, Shimo T, Yamashiro T, Takigawa M. (2013). Novel role of miR-181a in cartilage metabolism. *Journal of Cellular Biochemistry*, 114, 2094-2100.
- Takigawa, M., Tajima, K., Pan, H.-O., Enomoto, M., Kinoshita, A., Suzuki, F., Takano, Y. and Mori, Y. (1989). Establishment of a clonal human chondrosarcoma cell line with cartilage phenotypes. *Cancer Research*, 49, 3996-4002.
- Takigawa M. (2013). CCN2: A master regulator of the genesis of bone and cartilage. *J. Cell Communication & Signaling*, 7, 191-201.
- Takigawa M. (2017). The CCN proteins: An overview. *Methods in Molecular Biology*, 1489, 1-8.
- Tammimies, K., Bieder, A., Lauter, G., Sugiaman-Trapman D., Torchet, R., Hokkanen, M.E., Burghoorn, J., Castrén, E., Kere, J., Tapia-Páez, I., & Swoboda, P. (2016). Ciliary dyslexia candidate genes DYX1C1 and DCDC2 are regulated by Regulatory Factor X (RFX) transcription factors through X-box promoter motifs. *FASEB Journal*, 30, 3578-3587.
- Tsunoda, T., & Takagi, T. (1999). Estimating transcription factor bindability on DNA. *Bioinformatics*, 15, 622-630.

Legends to figures

FIGURE 1. Effect of NaF treatment on the expression of all of the human cellular communication network factor (CCN) family genes in human chondrocytic HCS-2/8 cells. Four independent HCS-2/8 cell cultures were treated with NaF at the indicated concentrations for 12 h. Relative expression levels against those of *ACTB* are shown. * $p < 0.05$ and ** $p < 0.01$ significantly different from the control.

FIGURE 2. Impacts of starved conditions on CCN2 and CCN3 expression in human chondrocytic HCS-2/8 cells. **(a)** Reduction of CCN2 expression by glucose starvation for 48 h in HCS-2/8 cells. Six independent cultures were evaluated for each group. Relative expression levels against the control with glucose are plotted. **(b)** Dose-dependent induction of CCN3 by NaF treatment. Four independent HCS-2/8 cell cultures were treated with NaF at the indicated concentrations for 24 h. **(c)** CCN2 repression and CCN3 induction by MIA treatment. Four independent HCS-2/8 cell cultures were treated with 4 $\mu\text{g/mL}$ of MIA for 12 h. **(d)** Summary of the impacts of glycolysis deficiency on the CCN family expression. The results of this figure are summarized together with previous findings (Akashi et al. 2018). Relative expression levels against those of *ACTB* are shown. * $p < 0.05$ and ** $p < 0.01$ significantly different from the control.

FIGURE 3. Induction of CCN3 by glycolysis inhibitors in breast cancer cells. Effects of monoiodoacetic acid (MIA) and NaF on CCN3 expression in highly metastatic MDA-MB-231 cells **(a)** and non-metastatic MCF7 cells **(b)**. Four or three independent MDA-

MB-231 or MCF7 cell cultures were treated with MIA or NaF, respectively, for 12 h at the concentrations indicated. Relative expression levels against those of *ACTB* were computed and are shown as mean values with standard deviations. * $p < 0.05$ and ** $p < 0.01$ significantly different from the control.

FIGURE 4. Mapping of an enhancer that mediates the *CCN3* regulation by glycolytic activity in the proximal promoter region of human *CCN3*. **(a)** Functional mapping by a reporter gene assay. Reporter plasmids containing firefly luciferase genes under the control of the *CCN3* proximal promoter fragments (shown at the top of the panel) were transfected into HCS-2/8 cells, and the promoter activity was assessed. Relative firefly luciferase activities standardized by *Renilla* luciferase activities from the internal control plasmid (pRL-TK) were computed from the data obtained from four independent cultures. Mean values are shown with error bars of standard deviations. ** $p < 0.01$ significantly different from the control. **(b)** In silico prediction of enhancer elements. Putative DNA sequences that could be targeted by known transcription factors were predicted by the TFbind online program and are indicated by gray and black boxes with the names of corresponding transcription factors.

FIGURE 5. Identification of regulatory factor binding to the X-box (RFX) 1 as a *CCN3*-binding transcription factor that is induced upon glycolysis deficiency. **(a)** Analysis of datasets downloaded from the ENCODE portal with the University of California Santa Cruz (UCSC) genome browser. The transcription factor chromatin immunoprecipitation-sequencing (ChIP-sequencing) data from MCF7 cells (ENCSR788XNX) and total RNA sequencing data from human articular chondrocytes

(ENCSR000CUE) were analyzed. Coverages around the *CCN3* locus (indicated at the bottom) are shown on the hg19 reference genome. **(b)** Induction of *RFX1* by glycolysis inhibition. Four independent HCS-2/8 cultures for each were treated with the indicated concentrations of MIA or NaF. **(c)** Effect of glucose starvation on *RFX1* expression in HCS-2/8 cells. Symbols "+" or "-" indicate the data from three independent cell cultures with or without glucose for 24 h (left panel) and 48 h (right panel), respectively. Data are standardized as the expression levels of *ACTB*, and mean values are shown, with error bars representing standard deviations. * $p < 0.05$ and ** $p < 0.01$ significantly different from the control.

FIGURE 6. *RFX1*-dependence of the *CCN3* induction by NaF in HCS-2/8 cells. **(a)** Experimental time course. In order to silence *RFX1*, the cells were transfected with a small interfering RNA (siRNA) cocktail for 24 h, which was followed by the extraction of RNAs and proteins after 16 h of NaF treatment. **(b)** Efficient silencing of *RFX1* (left panel) and inefficient induction of *CCN3* (right panel) by NaF in those cells. NaF treatment was performed at a concentration of 5 mM. Data represent mean values and standard deviations obtained from four independent HCS-2/8 cell cultures. ** $p < 0.01$ significantly different from the control. **(c)** Western blotting analysis of *CCN3* production in HCS-2/8 cells stimulated by 5 mM NaF after the transfection with a non-targeting siRNA control (siCont) and *RFX1*-targeting siRNA cocktail (siRFX1). As an internal control, the production of β -actin was also evaluated. Arrows on the right indicate respective proteins of interest. Positions of the molecular weight marker are shown in kilodaltons on the left.

FIGURE 7. Effect of an anti-CCN3 antibody on the viability of HCS-2/8 cells in the presence of NaF. **(a)** Experimental time course. Six independent cell cultures were first exposed to 5 $\mu\text{g}/\text{mL}$ of a non-immune IgG (IgG) or an antibody against CCN3 for 24 h, and were then treated with 5 mM NaF for an additional 24 h. **(b)** Evaluation of the viability of those cells via a WST assay. ** $p < 0.01$ significantly different from the control.

FIGURE 8. (a) Distribution of CCN3-producing cells in mouse developing epiphyseal cartilage at embryonic day 16. CCN3 in mouse tibial epiphyseal cartilage sections was immunohistochemically visualized in brown with an anti-CCN3 antibody (CCN3). Control sections were stained by normal goat antibodies. C, cartilage; and M, meniscus. Stronger signals can be observed in the deeper zones more distant from synovial fluid. Scale bars: 200 μm . **(b)** Schematic representation of the mechanism and possible role of CCN3 induction under starved conditions. Open thick arrow and solid thick arrows represent protein production and transcriptional activation, respectively. Dotted arrows indicate induction through unknown mechanisms.

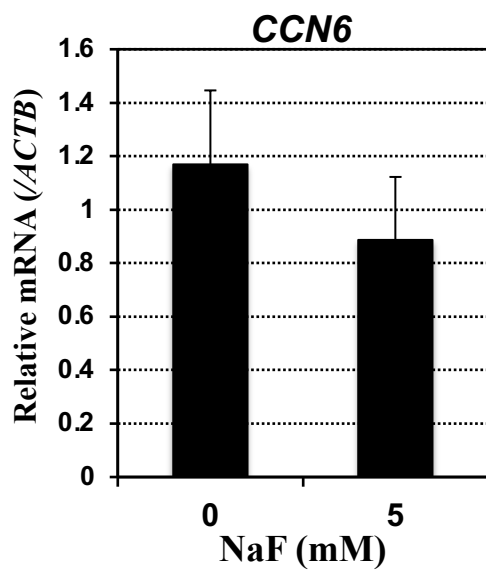
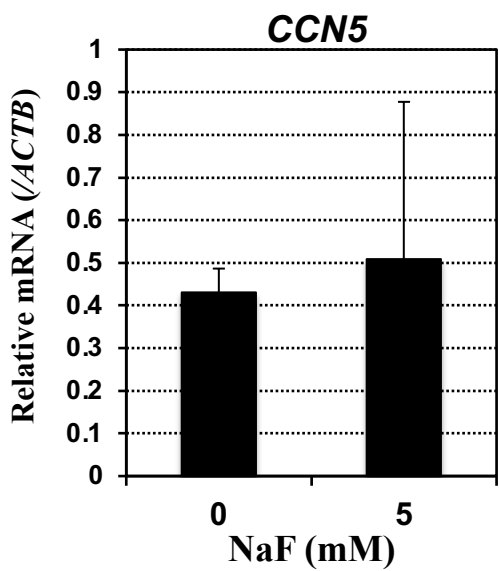
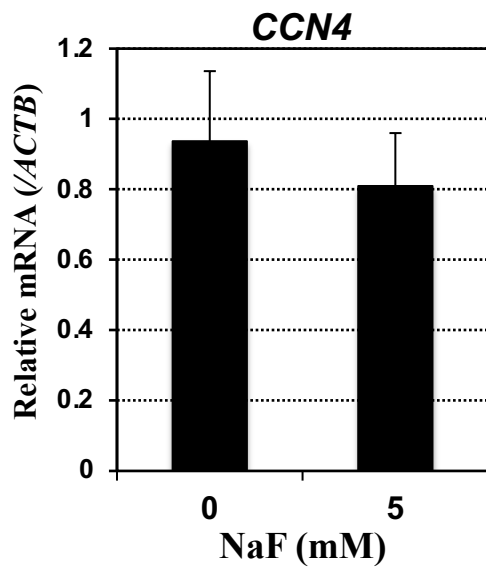
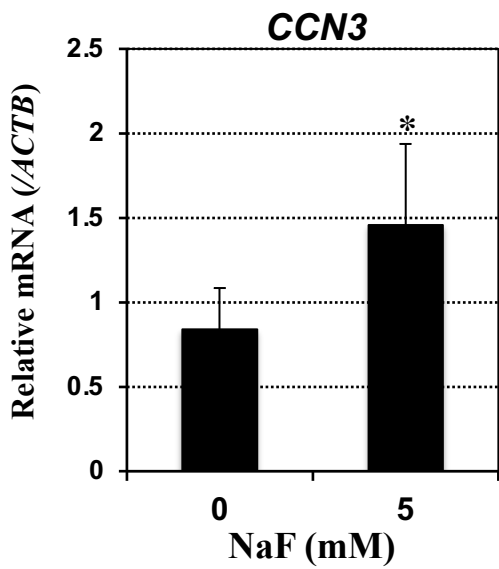
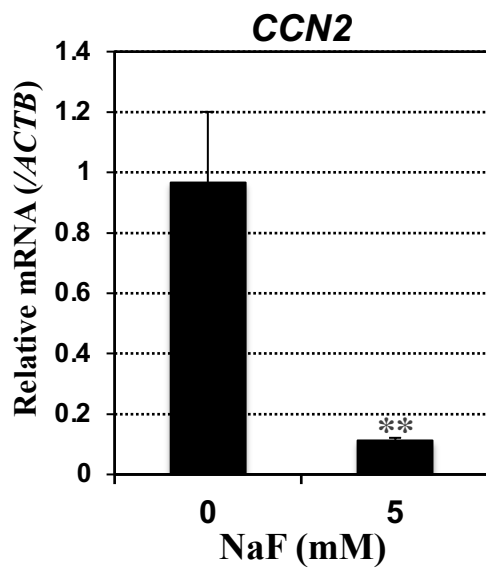
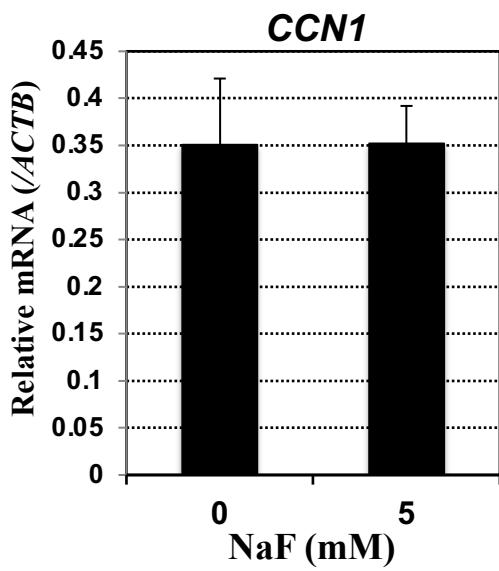


Figure 1. Mizukawa et al.

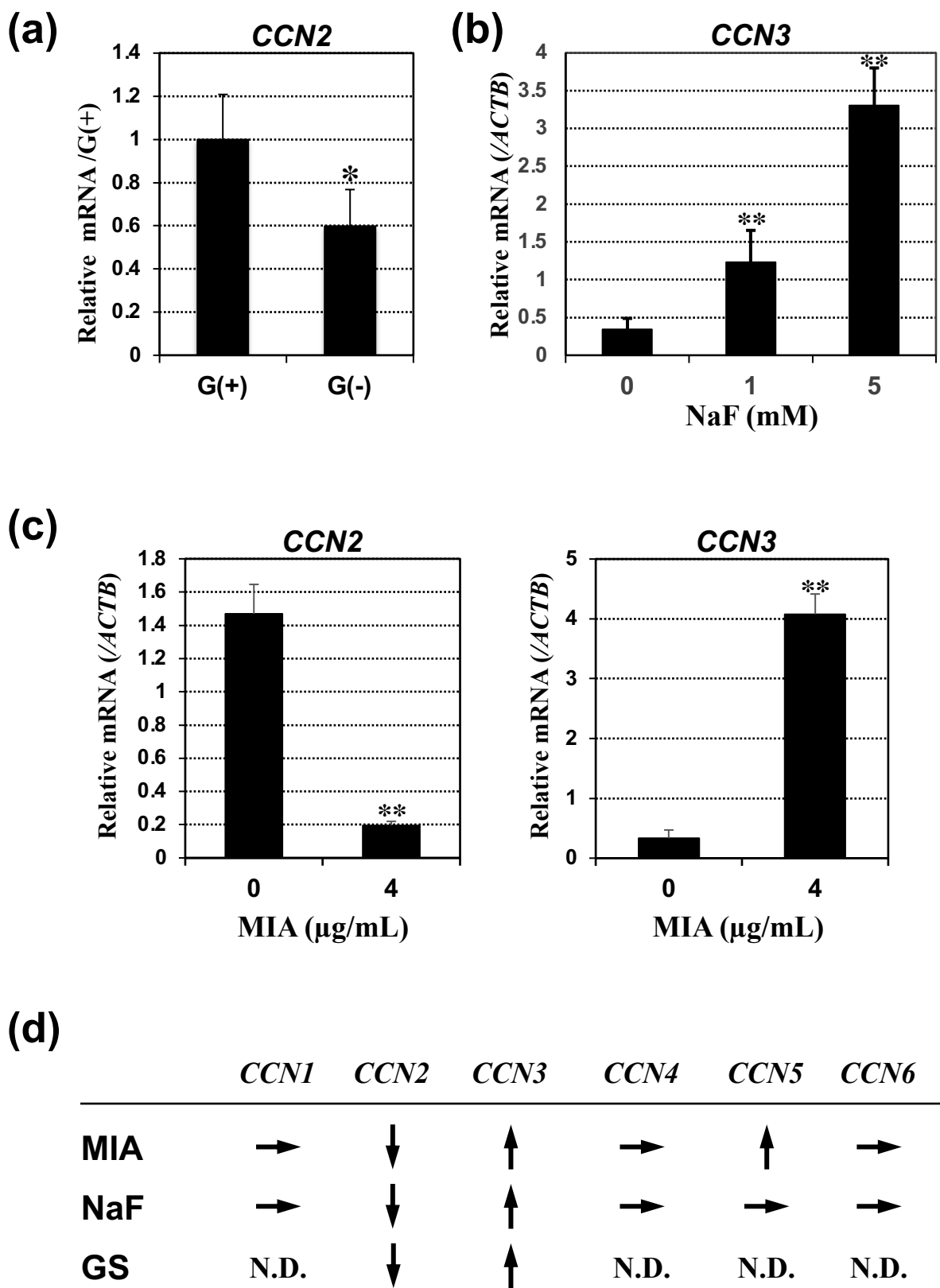


Figure 2. Mizukawa et al.

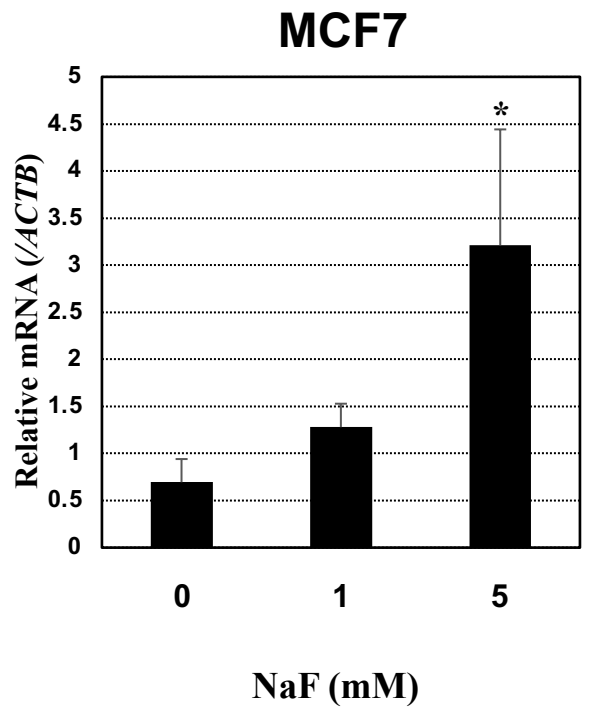
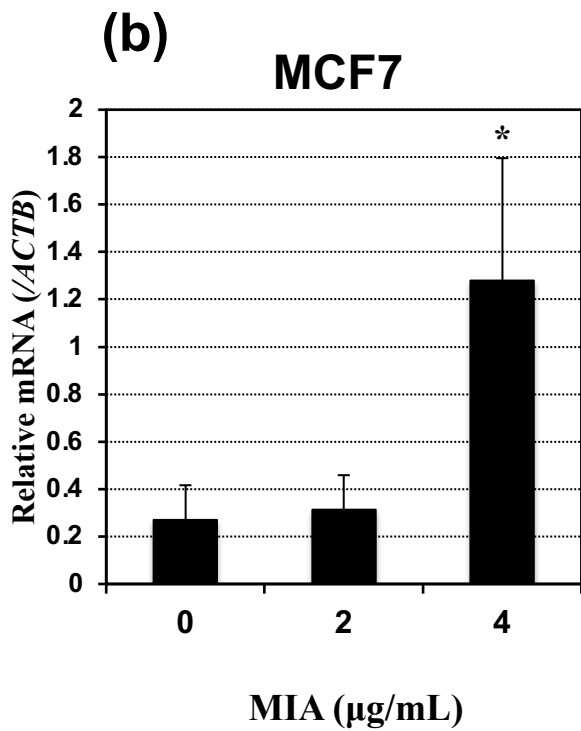
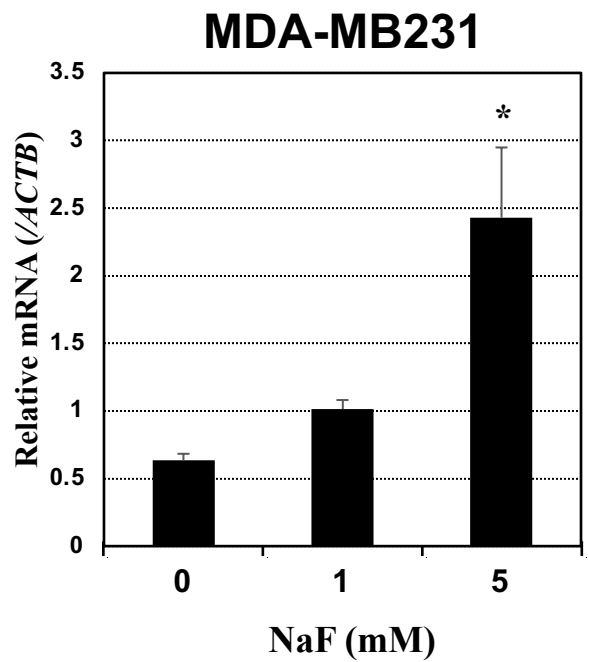
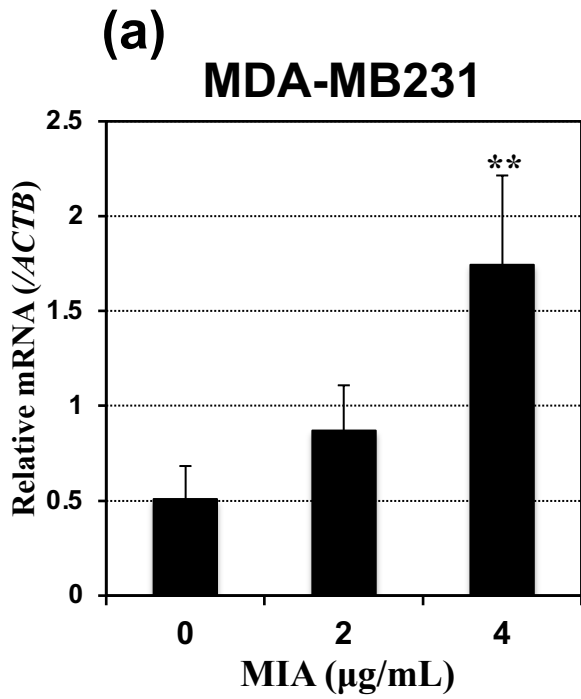
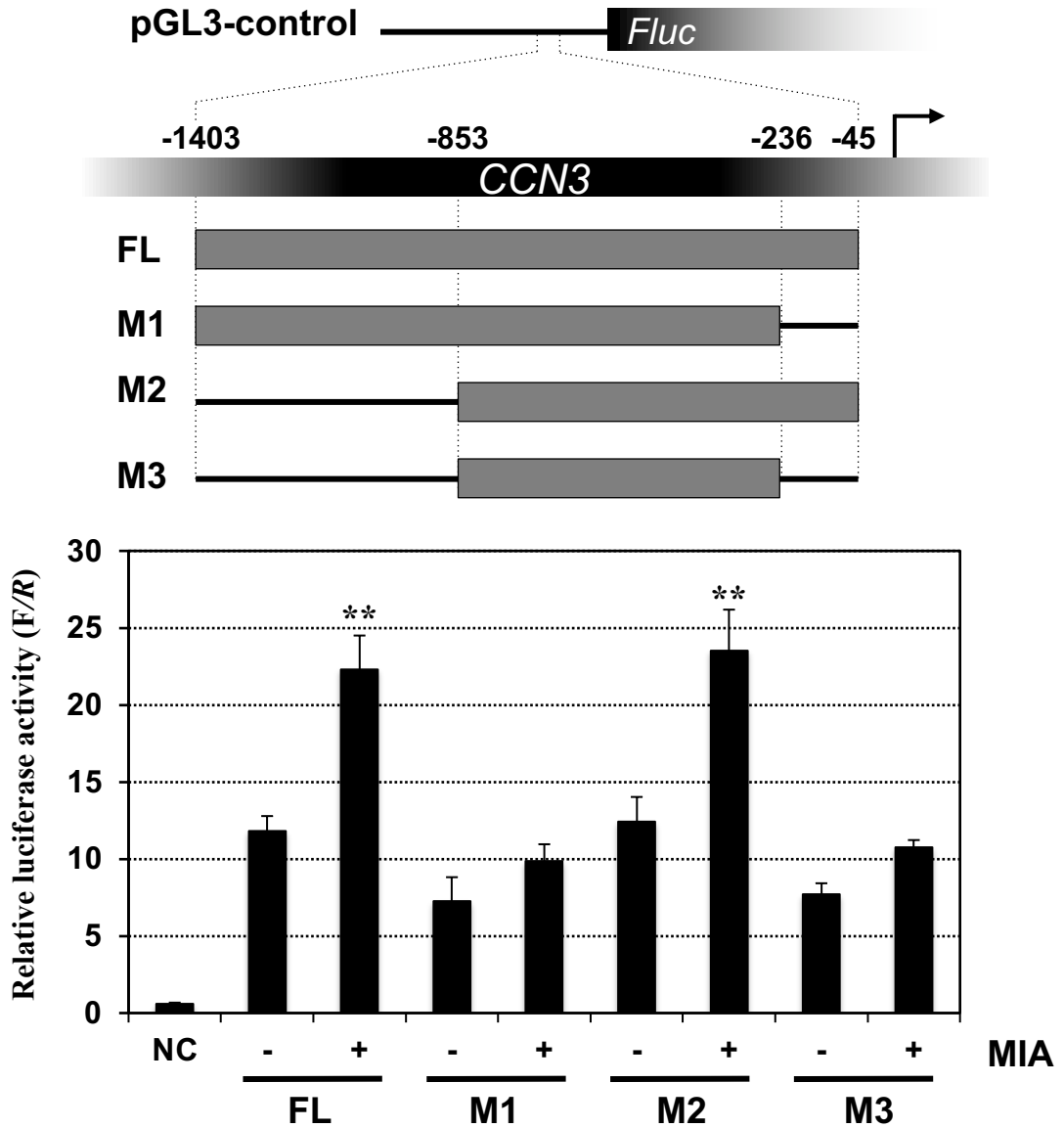


Figure 3. Mizukawa et al.

(a)



(b)

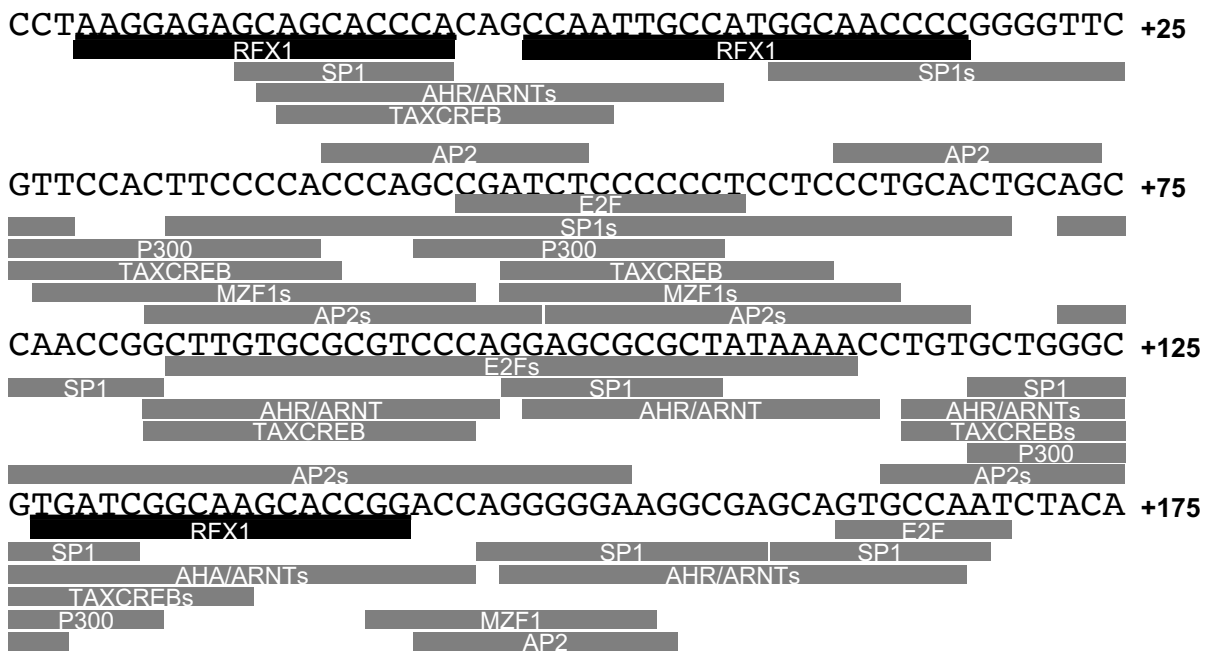
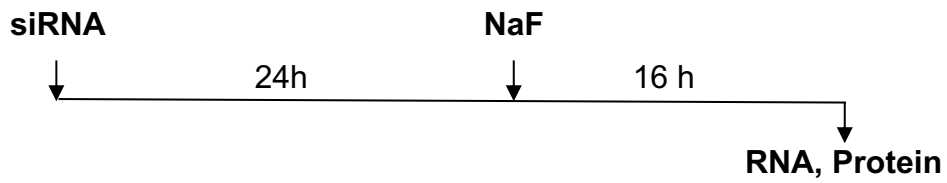
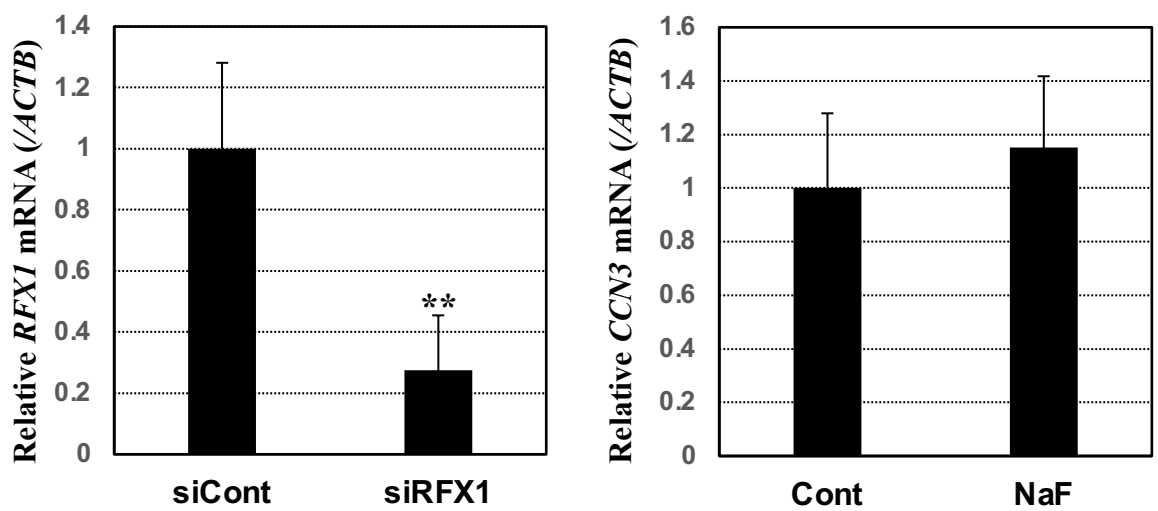


Figure 4. Mizukawa et al.

(a)



(b)



(c)

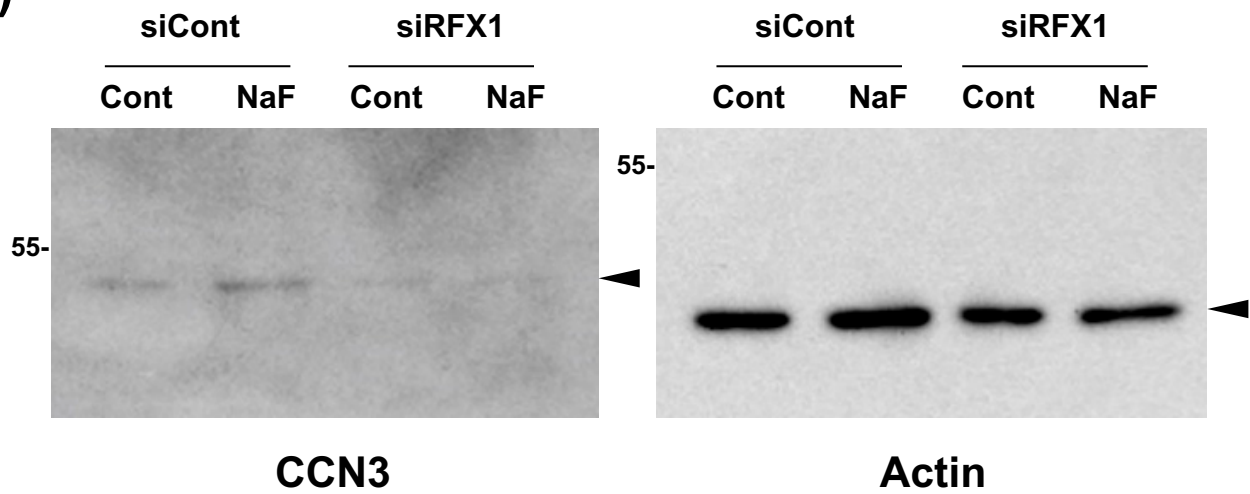
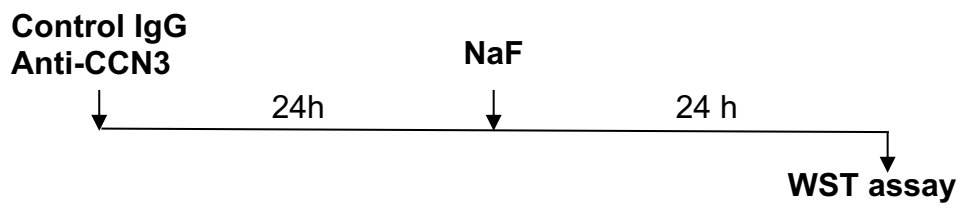


Figure 6. Mizukawa et al.

(a)



(b)

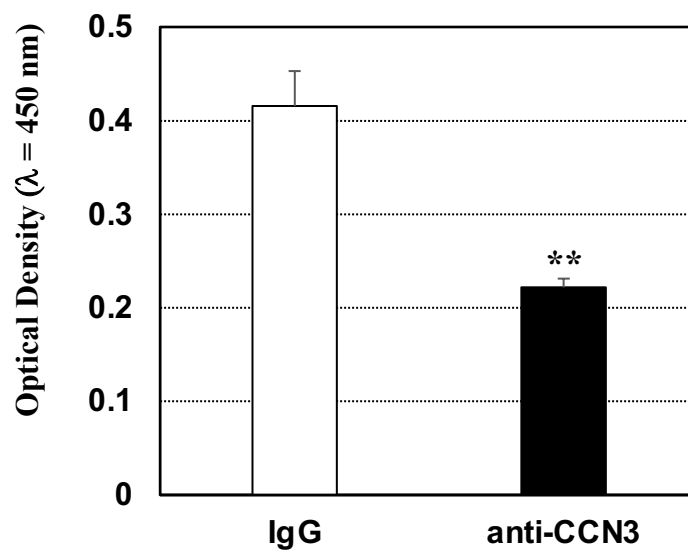
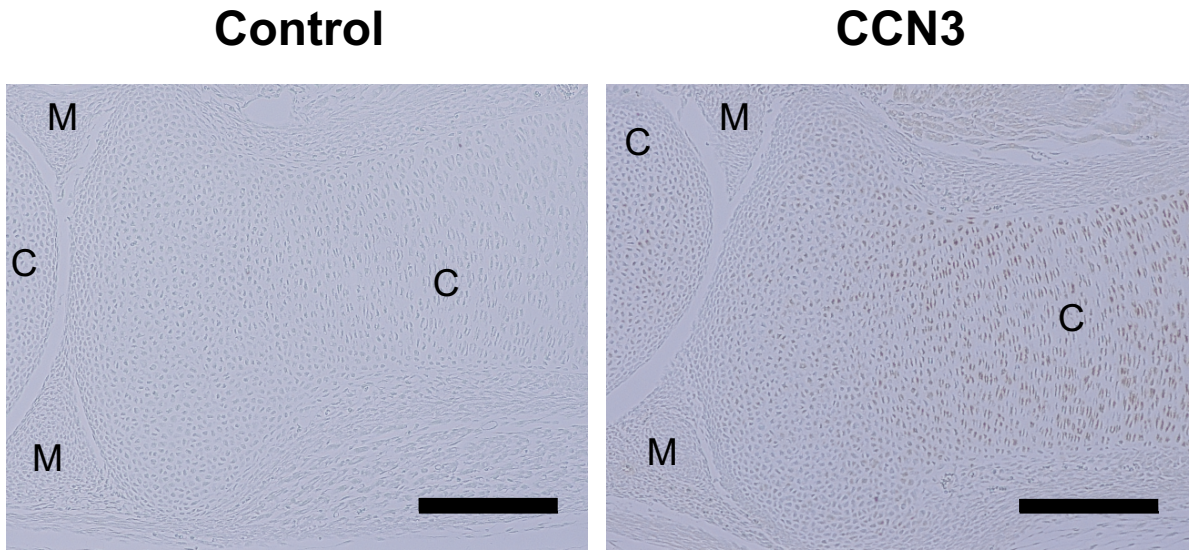


Figure 7. Mizukawa et al.

(a)



(b)

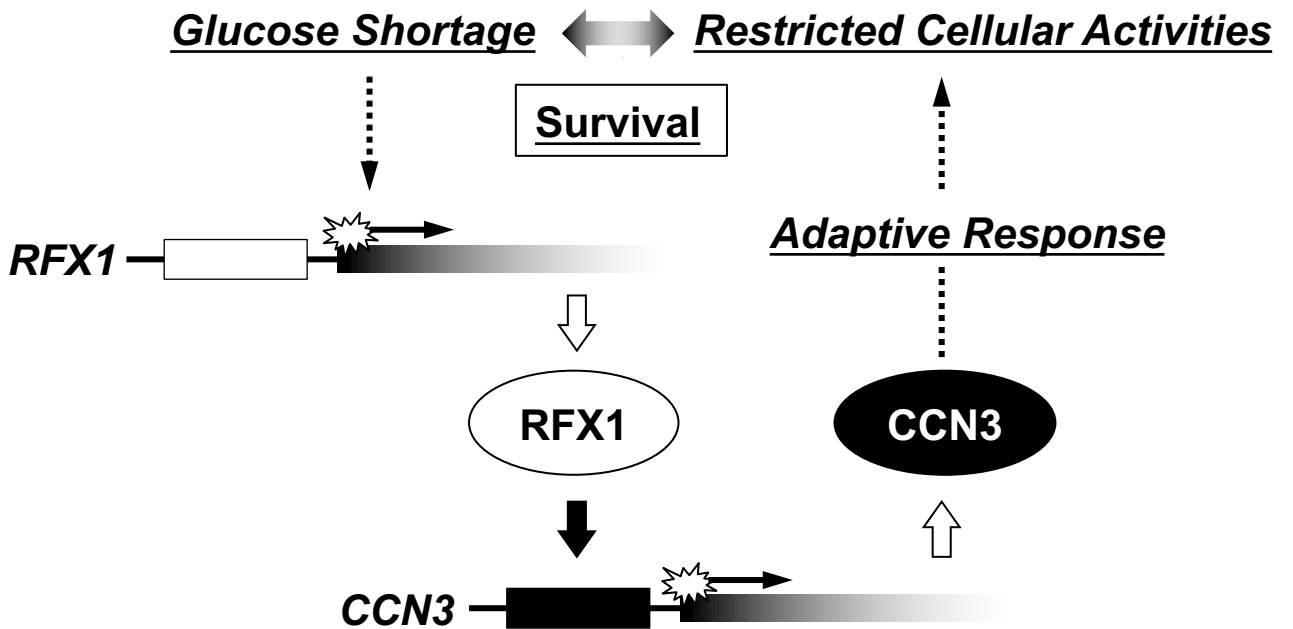


Figure 8. Mizukawa et al.

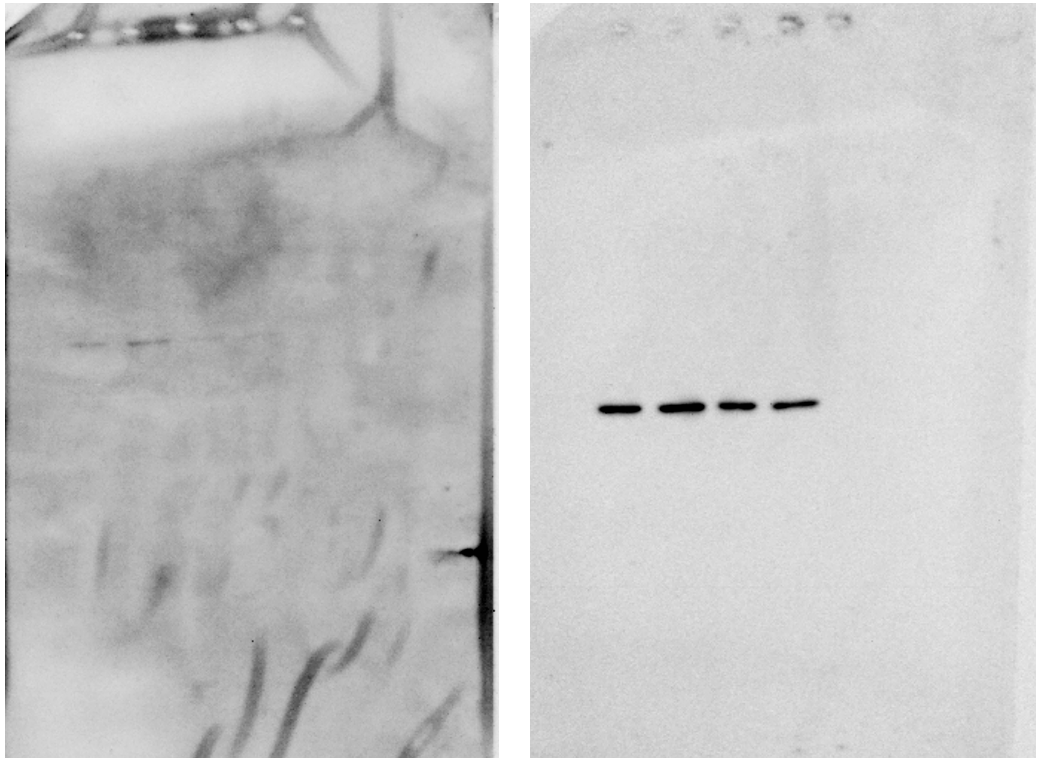


Figure S1. Original unprocessed images of Western blots shown in Figure 5(c).